ECG: design of an electrocardiograph and comparison with a numerical ventricular model

M. Ballesta[1], M. Guasch[1,2], and N. Salvat[1]

[1]ETSETB, Universitat Politècnica de Catalunya
[2]ETSEIB, Universitat Politècnica de Catalunya

Electrocardiology deals with the description of intracardiac bioelectric phenomena and the extracardiac electric field generated in the human body. It has been increasingly supported by the mathematical and numerical computational models. The formulation of models at both cellular and tissue levels provide essential tools in order to increase the knowledge of this phenomena. On the other hand, electrocardiography is the process which permits recording this electrical activity of the heart over a period of time using electrodes placed on the skin. This article presents a computational model of the heart that is compared with an electrocardiogram obtained in the laboratory using an electrocardiograph of own construction.

I. INTRODUCTION

The heart is a double pump consisting of four chambers, two atria in the upper and two ventricles in the lower part. The ventricular walls are externally lined by a thin connective layer called epicardium and internally by the endocardium, with the cardiac muscle called myocardium in between. The main cardiac functions, pulmonary and systemic circulation, are due to the contraction of heart, which is coordinated by its electrical activity. The contraction of cardiac cells is initiated by an action potential, when a depolarizing transitory membrane current raises the transmembrane potential from its resting value (approx. -80 mV) to slightly positive values followed by a repolarizing current that returns the transmembrane potential to its resting value.

The electrical activity of the heart originates at the sinoatrial node (SAN) a group of cardiac pacemaker cells located on the right atrium. In normal conditions SAN cells generate an action potential that propagates throughout the right atrium to the left atrium stimulating the myocardium of both atria to contract. The activation front reaches the atrioventricular node (AVN) that conducts the action potential through the atrioventricular septum, activating the specialized fibers of the Bundle of His and the Purkinje network that spread as a tree-like left and right bundle branches ending on the endocardial surface of the ventricles. These Purkinje terminations transmit the action potential to the ventricular walls and cardiac excitation then propagates throughout the ventricles.

The registration of the extracellular potential on the body surface due to the propagation of cardiac action potential is known as electrocardiogram (ECG). The various deflections in the ECG signal are denoted as P, Q, R, S, T (see Fig. 1). The P wave is associated with atrial depolarization while the PQ segment is the delay between the beginning of atrial and ventricular activation. The subsequent QRS complex is associated with the complex
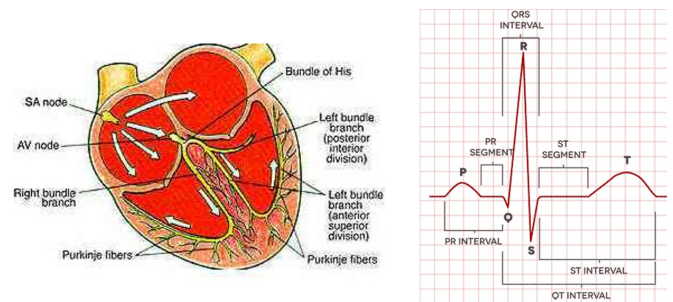

FIG. 1. Schematic diagram of the heart conduction system [2] and ECG waveform

activation sequence of the ventricles resulting in upwards and downwards deflections. The Q wave correspond to the activation of the interventricular septum and the S wave shows the activations of the ventricular free walls. The QRS complex is followed by a rather long period where all the cells are depolarized. Finally, the T wave signals ventricular repolarization and its morphology depends on the repolarization sequence through the ventricles. [1]

II. METHODS

A. Electrocardiograph

An electrocardiograph is an electrical instrument that detects and records minute differences in electric potential signals (about 1mV) occurring between different parts of the body caused by heart action. In a conventional ECG machine 10 electrodes are placed on the patient. This conformation forms a 12-lead system where each lead is a comparison between two electrodes. In this way, it is possible to present 12 different perspectives of the heart electrical activity from different angles. The graph of voltage versus time produced by this procedure
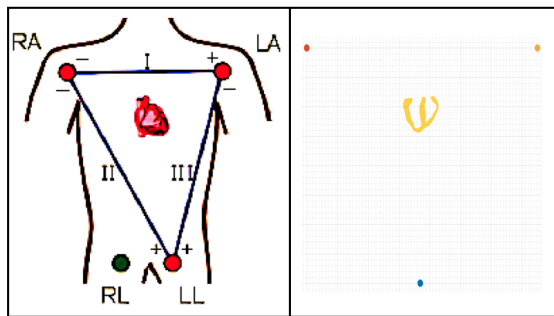
FIG. 2. On the left, general schematic representation for lead I, lead II and lead III. On the right, position of the electrodes used on the numerical model: blue (69,65,-500), red (300,65,300) and yellow (450,65,300). Although these coordinates depend on the precise collocation of the electrodes and one should, as well, take into account the inclination of the heart, the variation is small, with practically no impact on the ECG.

is the ECG.

Besides the standard 12 lead ECG a couple of variants could be used. The ECG machine that we have designed in the laboratory has only one lead. It is based on the limb lead I (see Fig. 2), i.e. the voltage difference between the (positive) left electrode (LA) and the (negative) right electrode (RA). The electrode (RL) on the right leg serves as a reference electrode for recording purposes. Lead I gives information of the electrical activity from the vantage point of the lateral wall of left ventricle. Thus, it was expected to observe the QRS complex and the T wave in the ECG recorded using it.

Fig. 3 shows the block diagram of the system designed. It is based in four main elements: an instrumentation amplifier (INA118), a microcontroller board (Arduino Leonardo), a galvanic isolator (optocoupler ILD615-3) and a USB TTL Serial cable (FTDI TTL-232RG).

One of the fundamental component for an electrocardiograph is the Instrumentation amplifier (IA). ECG voltages measured across the body are on the order of hundreds of microvolts up to 1 mV. This low voltage needs a low noise circuit, that is why instrumentation amplifiers are the key. Basically, an IA is a differential amplifier circuit that provides high input impedance and high gain. Since many error sources are common-mode, the use of a differential amplifier allows one to greatly reduce the noise of the signal. For this reason they can extract and amplify weak signals out of the noisy environment and feed a clean single-ended output [3]. That is why we have used it to take the voltage difference between leads (where the LA and RA electrodes are placed, as can be seen in Fig. 4).

The output signal V_0 for the INA118 [3] is:

$$V_0 = G(V_{in}^+ - V_{in}^-) + V_{ref} \qquad (1)$$

where the gain [3] is $G = 1 + \dfrac{50k\Omega}{R_g}$

Then, the output signal is converted to digital by the ADC of the microcontroller. Our microcontroller works at 330Hz to sample the analogue signal provided by the IA. In general, the frequency spectrum of an ECG signal does not have components above the 60 Hz on healthy patients. Thus, the Nyquist frequency is about 120Hz and aliasing effects in the signal are not expected.

Safety features are the most important elements in the system. An electrocardiograph is an instrument directly connected to a human body. Since parts of the machines are powered by the electrical grid, it is conceivable that either person could be subjected to intensity capable of causing death. Thus, isolating methods must be used. For example, electrodes are connected to the circuit by high impedance lines. This isolation may be enough in normal conditions. However, the system must be safe in case of failure too. In order to accomplish this requirement some other techniques are needed. The most effective one is the use of a galvanic isolation. It is a principle of isolating to prevent current flow: no direct conduction path is permitted. Information can still be exchanged between the sections by other means, such as optical ones [4]. We have used an opotocoupler to perform this action.

Optocouplers are components that transfer electrical signals between two isolated circuits by using light. Our optocoupler consists of a LED (emitter), that converts electrical input signal into light, and a photo-transistor (receptor) (see Fig. 5) which detects incoming light and either generates electric energy directly, in the same opaque package. These two elements must have different power supplies and different grounds. In this way, the circuit connections to each of them are totally isolated. Low supply voltages are used on the side that is connected to the body and electric grid supplies the other side.

The signal after the optocoupler, which carries all the collected data, is finally sent to the PC through a serial TTL to USB converter cable. When the cable receives a byte on the RX input line, it will send that byte to the computer via USB [5], as can be seen in Figure 5.

When operating, ECG records voltage differences between the electrodes. The signal we were obtaining was simultaneously send to the PC through the galvanic isolation. Then, those samples could be treated and represented using MATLAB tools. Specifically, we used a box filter to reduce the noise.

B. Model

We have also calculated the ECG using an electrical wave propagation model. Even though a beat of the heart includes also mechanical aspects, such as the muscle contraction, and fluid dynamics, considering only the electrical aspects is a simple, but good enough option to explore how an ECG works.

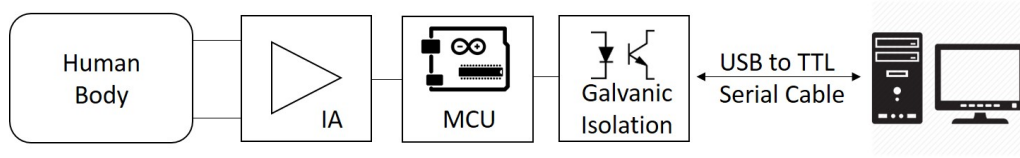To simulate properly the potential changes in myocar-

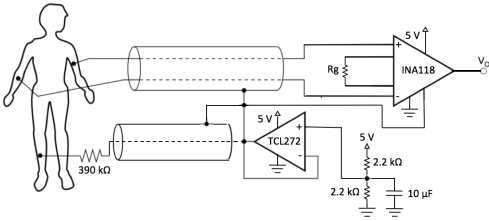FIG. 3. Block diagram of our electrocardiograph

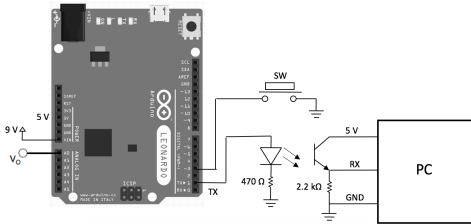FIG. 4. Our circuit, from human body to output voltage of the IA

FIG. 5. Our circuit, from the microcontroller to the PC

FIG. 6. Action potential for a ventricular cell.

diocytes, a model of the membrane electrical behaviour must be considered. A cell membrane consists of a phospholipid bilayer that differentiates intracellular and extracellular media, with different ion concentrations. On the membrane, there are proteins that act as ion channels or pumps, enabling ions to cross the membrane by active or passive transport.

On the other hand, the membrane also acts as a capacitor, accumulating charge. From the conservation of the global charge, the temporal evolution of an isolated cell potential can be found:

$$C_m \frac{dV}{dt} = -\sum_X I_X = -I_{ion} \qquad (2)$$

The current I_{ion} presents complex dynamics, whose basics are shown in Fig. 6. There are plenty of different models for I_{ion}, mostly based on Hodgkin and Huxley description, as the one used in this paper, which considers only Na, K and Ca currents [6]. In addition, it has been shown experimentally that cells from the endocardium and epicardium have slightly different behaviours, having the former a shorter action potential, although in our model these differences are not contemplated.

Now, using the cable equation [7], one can consider the adjacent cells and generalize this model to a 3D formulation. The final equation governing the dynamics of the cell potential is:
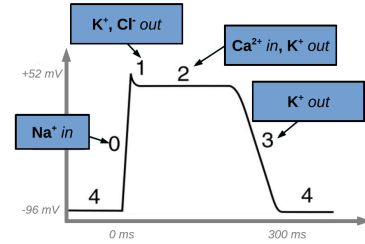
$$\frac{\partial V}{\partial t} = \frac{-I_{ion}}{C_m} + \nabla \cdot (D\nabla V) \qquad (3)$$

with a no-flux boundary condition:

$$\hat{n} \cdot D\nabla V = 0 \qquad (4)$$

where $\hat{n}$ is the unit vector normal to the boundaries of the ventricles and D represents the diffusion tensor.
In order to model the anisotropic behaviour, D can be assumed different for the perpendicular plane to the fiber and the parallel one, such that

$$D\nabla V = D_\perp \nabla V + (D_\parallel - D_\perp)\hat{\tau} \cdot \nabla V \qquad (5)$$

where $\hat{\tau}$ is the direction parallel to the fiber.

The values taken for $D_\parallel$ and $D_\perp$ are the same used in [6], $1.2 \cdot 10^{-3} cm^2/ms^{-1}$ and $0.3 \cdot 10^{-3} cm^2/ms^{-1}$ respectively.

The implementation of the boundary condition (4) is achieved through an auxiliary function, ϕ, that takes a value of 1 or 0 for points belonging to the heart tissue or not, respectively. Now, Eq. 3 can be rewritten:

$$\frac{\partial V}{\partial t} = \frac{-I_{ion}}{C_m} + \nabla \cdot (\phi D\nabla V) \qquad (6)$$

This differential equation is solved using finite differences and a simple Euler method, with a discretization of $\Delta x = \Delta y = \Delta z = 0.025cm$ and a time step $t = 0.1ms$.

As for the geometry of the ventricles, we use a rabbit heart model, described in [8]. The same model is used to define a set of points with special properties, all located in the same plane, which represent the Purkinje fibers. Here, we have manually implemented the behaviour of these cells. First, we excite the Purkinje cells of each ventricle, with a small delay between them and then we set a propagation speed of 300 cm/s along the fibers.
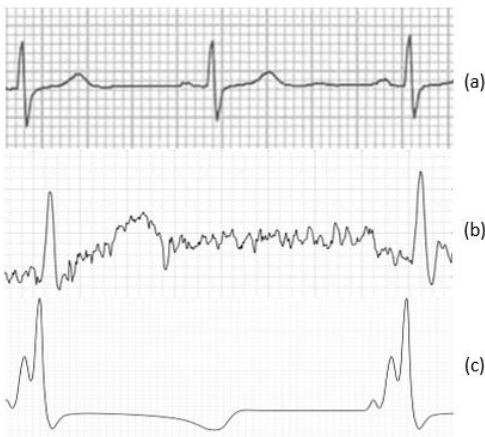
FIG. 7. ECG extracted from medical sources (a)[9]; ECG obtained from electrocardiograph designed in the laboratory (b); ECG of the I lead obtained from the simulations (c)
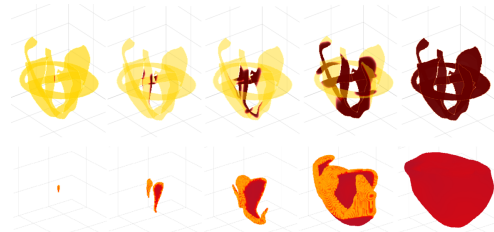

FIG. 8. Depolarization processs, represented by two different methods. Each column represents the same time instant. Above, a slice graphic for three representative planes, including the one containing the Purkinje fibers. Here, all the heart tissue is plotted. Yellow represents those regions with still a resting potential, while a more reddish colour means a higher potential value. Below, a 3D representation where the lattice points get coloured as the action potential spreads. Orange is for smaller values of the potential, while red corresponds to the maximum value the potential can take.

Once defined the mathematical model used to simulate the propagation of the electrical wave, we can get the external potential of any position like

$$V(x_0, y_0, z_0) = \int \frac{\nabla \cdot (\phi D \nabla V) dx dy dz}{\sqrt{(x - x_0)^2 + (y - y_0)^2 + (z - z_0)^2}} \tag{7}$$

Defining the relative position of the electrodes, we can calculate any lead using Eq. 7. In this paper, and with the comparison with the electrocardiograph results in mind, we define only three electrodes - Einthovens triangle (see Fig. 2).

III. RESULTS

Our ECG machine was implemented with cooper coins as electrodes. The tester volunteers were placed in front of the instrument with one electrode per arm. The electrode of the right leg were also necessary to level the reference of the person with the reference of the electrocardiograph. Fig. 7 (b) shows a representative electrocardiogram obtained in the laboratory.

Regarding the model, for this project, we aimed at obtaining not only a simulated ECG, as accurate as possible (see Fig. 7), but also to create a visualisation of the electrical wave propagation. As the heart model is a 3D geometry, we have opted to represent the potential as colours, using a gradient from yellow to red (see Fig. 8).

Thanks to this visual representation, one can easily see how both the depolarization and repolarization of the heart travel from the endocardium to the epicardium. While for the depolarization it is, indeed, accurate, this is not the case for the repolarization. This misbehaviour is due to the fact that the action potential of the Purkinje fibers is longer than the rest, as previously mentioned. In consequence, during repolarization, we get the inverted potential or, from an ECG point of view, we get a nega-tive T-wave (see Fig. 7).

IV. DISCUSSION AND CONCLUSIONS

Each image of Fig. 7 is an ECG of the limb lead I. The potential differences that they capture only can provide the information of the QRS complex and T wave. Image (a) is a true clinic ECG of lead I and it shows three QRS complexes and three T waves. In (b), the experimental ECG, it can be easily appreciated the presence of the QRS complex: it is the sharp peak that rises and falls quickly and then reestablished. T wave is more difficult to detect due to the presence of noise in the process of sampling. Still, it can be seen a slight increase of the signal shortly after the first QRS complex. This matches with the T wave in (a). Finally, in the ECG obtained using the mathematical model, (c), the general outline of the QRS complex can also be observed. However, due to the nature of the model, both the Q and T wave appear inverted and the R peak becomes split.

In this paper we have reviewed briefly the basics of the electrical dynamics of the heart and used two different methods - experimental and numerical - to obtain an ECG, encountering difficulties in each one of them. For construction of the ECG, we have met with difficulties along the reduction of noise and the obtention of a proper signal from the body while keeping the subject safe. As for the numerical simulation, the results were not as accurate as we expected, due to the limitations of the model. Further improvements could use a tensor to define the action potential for type of cell, in order to capture a more accurate T wave. The ionic model used or the location and excitation of the Purkinje fibers could also be upgraded. Finally, the solving of Eq. 6 could be implemented using a higher order method, like RK4, to minimize the numerical error while optimizing the computational cost.

[1] P. C. Franzone, L. F. Pavarino, and S. Scacchi, *Mathematical cardiac electrophysiology*, vol. 13. Springer, 2014.

[2] "Cardiovascular system/ heart and blood vessels." `http://kathytbiology.blogspot.com.es/2008_09_28_archive.html`.

[3] Texas Instruments, *Precision, low power instrumentation amplifiers*, 1998.

[4] P. Hasse, *Overvoltage protection of low-voltage systems*, vol. 33. IET, 2000.

[5] FTDI Chip, *TTL to USB Serial Converter Generic Cables Datasheet*, 2005.

[6] B. Echebarria and A. Karma, "Mechanisms for initiation of cardiac discordant alternans," *The European Physical Journal Special Topics*, vol. 146, no. 1, pp. 217–231, 2007.

[7] J. Keener and J. Sneyd, *Mathematical physiology*, vol. 1. 1998.

[8] F. Vetter and A. McCulloch, "Prog. biophys.," *Mol. Biol.*, no. 69, p. 157, 1998.

[9] "Normal 12 lead ecg." `http://ecg.utah.edu/img_index`.